Int. J. Heat Mass Transfer. Vol. 21, pp 1481–1490

0017-9310/78/1201-1481 $02.00/0

AN EXPERIMENTAL INVESTIGATION OF NATURAL CONVECTION FLOW ON AN INCLINED SURFACE

HUSSAIN SHAUKATULLAH and B. GEBHART
Mechanical Engineering Department, State University of New York at Buffalo, Buffalo, NY 14214, U.S.A.

(*Received* 27 *September* 1977 *and in revised form* 28 *April* 1978)

Abstract—A thermocouple and two hot-film anemometer probes in the form of an "inverted V" were used to investigate the boundary region flow formed over an inclined surface dissipating a uniform heat flux. Temperature and the longitudinal and transverse components of velocity were measured. A single longitudinal vortex system arises. It causes a spanwise variation of the temperature and velocity fields, which results in a spanwise variation of heat transfer. The spanwise mean-flow variation, or vortex system, arises first downstream for angles greater than 11°. Our local measurements permit detailed comparison with well-established disturbance mechanisms in vertical flows. Frequency filtering of periodic disturbances is again found. The beginning of transition is postulated in terms of disturbance magnitude. The location is found to depend on the distance from the leading edge, in addition to the Grashof number, in the same way as in vertical flows.

NOMENCLATURE

B^*, characteristic frequency $= 50\pi f x^2/\nu G^{*2.5}$;
c, specific heat of water;
E, transition factor;
f, frequency [Hz];
f', non-dimensional form of velocity $= 5xu/\nu G^{*2}$;
$\bar{f}'_z$, RMS value of f' variation in spanwise direction;
g, acceleration due to gravity;
G, modified Grashof number $= 4(Gr/4)^{1/4}$;
G^*, modified flux Grashof number $= 5(Gr^*/5)^{1/5}$;
Gr, Grashof number $= g\beta(T_0 - T_\infty)x^3/\nu^2$;
Gr^*, flux Grashof number $= g\beta q'' x^4 \cos\theta/k\nu^2$;
h, heat-transfer coefficient;
k, thermal conductivity of water;
Nu, Nusselt number $= hx/k$;
Pr, Prandtl number $= \mu c/k$;
q'', heat flux to plate;
T, temperature in boundary layer;
T_0, temperature of plate surface;
T_∞, ambient temperature;
U^*, characteristic velocity;
u, tangential velocity component in boundary layer;
v_∞, entrainment velocity;
w, spanwise velocity component in boundary layer;
x, distance from leading edge of plate;
y, distance measured in boundary layer normal to plate;
z, distance measured in boundary layer parallel to plate.

Greek symbols

β, coefficient of thermal expansion of water;
η, non-dimensional form of distance in boundary layer $= yG^*/5x$;
θ, inclination of plate surface from vertical;
λ, vortex wave length;
μ, dynamic viscosity of water;
ν, kinematic viscosity of water;
ϕ, non-dimensional form of temperature difference $= (T - T_\infty)kG^*/5xq''$;
$\bar{\phi}$, spanwise average of ϕ;
$\bar{\phi}'_z$, rms value of ϕ variation in spanwise direction.

1. INTRODUCTION

NATURAL convection flows adjacent to flat inclined surfaces first were visualized by Schlieren, see Schmidt [1]. Rich [2] measured heat transfer at angles of inclination θ up to 40° from vertical, using a Mach–Zehnder interferometer. These results indicated that the heat transfer is within 10% of the values for vertical if the Grashof number is multiplied by the cosine of the angle of inclination. Subsequent studies of Vliet [3], Hassan and Mohamed [4], Lloyd, Sparrow and Eckert [5], Fujii and Imura [6], Vliet and Ross [7] and Black and Norris [8] have all supported this suggestion of Rich.

Kierkus [9] and Riley [10] used a perturbation method to solve the boundary-layer equations for inclinations up to 45° on either side of vertical. Kierkus found good agreement between calculations and experiments, using a Mach–Zehnder interferometer to measure temperature and dust particles to measure velocity. Lee and Lock [11] solved the boundary-layer equations numerically, for air, for inclination angles from 90° to −30° from vertical. Positive angles apply to a hot surface facing up. For angles up to 30°, the inclination has a very slight effect on velocity and temperature profiles.

The first experiment to investigate the instability

of such flow was that of Lock, Gort and Pond [12]. A schlieren and a thermocouple probe were used. Waves were seen. They determined critical Rayleigh numbers for incipient instability for inclinations from 60° to −80° from vertical. The results were not symmetric about 0°. Subsequent investigators have used various criteria to determine the end of laminar flow.

Sparrow and Husar [13] first demonstrated the presence of longitudinal vortices over an isothermal inclined surface in water. An electrochemical flow visualization technique was used. For angles of inclinations of 15° or more from vertical, longitudinal vortices were observed downstream of leading edge. The size of these vortices was found to be independent of the angle of inclination, but strongly dependent on overall temperature difference between the surface and ambient. Lloyd and Sparrow [14] continued these experiments to study the mode of instability at different angles. Below 14° waves were found to be the mode of instability, above 17° it was longitudinal vortices, and between 14° and 17° both were found to coexist. Lloyd [15] repeated the flow visualization experiments of Lloyd and Sparrow [14] and confirmed that the vortex wavelength is independent of inclination and depends on the temperature difference. Lloyd, Sparrow and Eckert [5] observed spanwise mass-transfer variation in the transition region for angles greater than 15° from vertical. Recently six linear analyses [16–21] for neutral stability have appeared for inclined flows generated over isothermal surfaces.

There have been many investigations of stability and disturbance growth in vertical flows. Earlier ones have been reviewed by Gebhart [22]. In a more recent experimental study, Jaluria and Gebhart [23] investigated the behavior of controlled two-dimensional disturbances, with a super-imposed transverse variation, in water, adjacent to a uniform flux surface. Interactions among these two disturbance modes led to the establishment of a secondary mean flow consisting of a double longitudinal vortex system. The experimental results were in agreement with the stability analysis of Audunson and Gebhart [24], which postulates a two-dimensional disturbance, modulated by a standing transverse disturbance.

Godaux and Gebhart [25] made a study of natural transition for a uniform flux surface condition, in water. This demonstrated quantitatively that transition is not accurately predictable solely in terms of the local Grashof number. Jaluria and Gebhart [26] confirmed this and found that the beginning of transition was correlated by a parameter in the form $G^*/x^{0.4}$. It was found to approximately correlate data for fluids with a wide range of Prandtl numbers, for both uniform flux and uniform temperature surface conditions.

Most studies of flow adjacent to inclined surfaces have been either heat-transfer measurements or visualization. To better understand the nature of instability in such flows, detailed local measurements in the boundary layer are necessary. These can supplement and extend the understanding gained from past observations. This was the aim of this study. A uniform flux surface, quite similar to the one used by Vliet and Liu [27], was used in experiments in water. Measurements in the boundary region were made using a thermocouple and two hot-film probes.

2. EXPERIMENTAL APPARATUS AND PROCEDURE

The experiments were done in a well-insulated tank of dimensions 66 × 68 × 91 cm high, with glass side walls. The distilled water was periodically deareated by spraying it into a bottle maintained at a vacuum of 50 cm of mercury. It was then filtered to 0.2 μm particles. A thermometer graduated to 0.1°C was used to measure the bulk temperature of water. Any stratification in the tank was dissipated by using a stirrer. Five copper–constantan thermocouples were placed at heights of 15, 45, 65, 75 and 85 cm from the bottom of the tank to indicate any stratification.

The uniform flux surface consisted of a 0.00127 cm (0.0005 in) thick sheet of Inconel 600 bonded to one side of a Teflon impregnated fiber glass fabric, by heating under high pressure. The total thickness of the sheet was about 0.009 cm, and had dimensions of 30 wide × 61.3 cm high. This bonded foil was pasted on a 2.5 cm thick extruded polystyrene insulation using two layers of 0.011 cm thick two-sided adhesive tape. Copper–constantan thermocouples made from 0.0126 cm (0.005 in) dia. wire were embedded between the two layers of tape. These were placed along the vertical centerline and also across the plate. The insulation supporting the foil was fixed to a 1.3 cm (0.5 in) thick acrylic plastic sheet which was supported in a stainless steel frame. Surface inclinations were possible to 30° from the vertical, with the heated surface facing up. These angles were measured by using an inclinometer graduated in 0.5° and further checked with the traversing mechanism. Glass plates 10 cm (4 in) high were installed on the sides of the heated surface, about 1.8 cm away from the edge, to minimize edge effects. An acrylic plastic plate, 10 cm long, was placed ahead of the leading edge of the heated section to act as an unheated starting length. A similar plate was placed at the trailing edge. During the experiments the leading edge was at least 13 cm above the bottom of the tank and the trailing edge 17 cm below the surface of water. The surface was heated by direct current through stainless steel electrodes. All plate and tank thermocouples used in ice bath as reference and were switched through a manual stepping switch.

Velocity measurements were made using constant temperature hot-film anemometers. The two calibrated hot-films were used in the "inverted V" arrangement, with the plane of V parallel to the surface. Calibrations were checked by measurement of velocity in the boundary layer with the surface

vertical, see Shaukatullah [28]. The separation between the centers of the films was 0.4 cm. Temperature in the boundary layer was measured using a chromel–alumel thermocouple made from a 0.00254 cm (0.001 in) dia. wire. The thermocouple bead was located in the plane of hot films and was 1.2 cm from the center of the V. This thermocouple also had a reference junction in an ice bath. A traversing mechanism capable of traversing in the three rectangular co-ordinate directions was used to position the probe assembly in the boundary layer. This mechanism had a resolution of 0.001 cm in the horizontal plane and a resolution of 0.002 cm in the vertical direction.

Surface heat flux was determined from the voltage drop across the surface and the current through a Leeds and Northrup 0.01 Ω resistance in series with the foil, using a digital voltmeter. Thermocouple and hot-film output were recorded on a chart recorder with four channels. Each channel had a recording width of 5 cm with 1 mm graduation. This amounts to a resolution of 2–4%. Data reduction was done with a computer program. Properties of water were evaluated at the film temperature, the average of the local surface and ambient temperature. The properties as functions of temperature were determined as follows: density and specific heat from Kell [29], thermal conductivity and viscosity from ASME steam tables [30].

Longitudinal and transverse velocities were calculated using the normal cooling cosine law. They were normalized by $U^* = vG^{*2}/5x$ where G^* is related to the local flux Grashof number $Gr_x^* = g\beta q'' x^4 \cos\theta/kv^2$ as follows, $G^* = 5(Gr_x^*/5)^{1/5}$. Temperature is nondimensionalized as $\phi = (T - T_\infty)kG^*/5xq''$ where T is the local temperature in the boundary layer and T_∞ is the ambient temperature. With this form, knowledge of the surface temperature is not required, except to evaluate properties. Distances across the boundary region are expressed as $\eta = yG^*/5x$. Spanwise locations are expressed in centimeters. The numbers are arbitrary. They are those on the scale of traversing mechanism. During data reduction the spatial separation of the probes was taken into account by taking spanwise traverses at 0.2 cm intervals over the central 4–6 cm of the plate. The output of each probe when it occupied the same location was used in the data reduction. Detailed information concerning experimental apparatus, instrumentation and procedure is given in Shaukatullah [28].

3. EXPERIMENTAL RESULTS

3.1. *Heat transfer*

This data was first obtained with the surface vertical, to check the overall validity of the equipment. The heat-transfer results were plotted in terms of the local Nusselt number $Nu = hx/k$ vs the Grashof number Gr^*. The data was in very close agreement with the vertical laminar boundary-layer result. A similar comparison for the plate inclined at 29° from the vertical, in Fig. 1 is much more interesting. The Grashof number is modified by cosine of the angle of inclination. The data agrees very well with theory for Gr^* to 2×10^{10}, then it diverges above. Similar results were found at smaller inclinations.

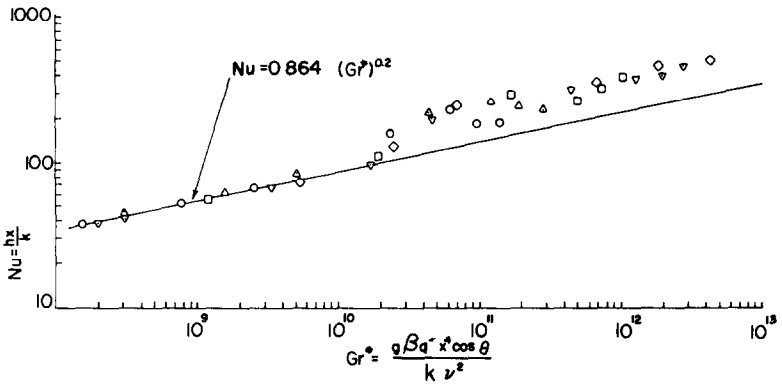

FIG. 1 Heat-transfer data for 29°. For heat fluxes of ⊙ 377 W m^2, △ 811 W/m^2, ⊡ 2291 W/m^2, ▽ 5049 W/m^2, ◇ 7081 W/m^2 —— Laminar boundary-layer solution for vertical flow at $Pr = 6.0$.

Upon beginning probes of the boundary region, we discovered that all but five of the thermocouples embedded in the surface, at distances of 2.5, 5, 10, 20 and 45 cm from the leading edge, were inoperative due to corrosion of the leads. For subsequent experiments the surface temperature used for evaluating water properties was approximated by interpolating between the temperatures indicated by these thermocouples. The output of these remaining thermocouples was frequently checked. They continued to function properly.

3.2. *Temperature measurements*

Figure 2 shows typical spanwise mean temperature measurements in the boundary layer for $\theta = 19°$ and at a fixed distance y and heat flux q'', at various downstream locations x. A spanwise variation gradually arises and increases downstream. It remains almost periodic across the surface, at the same wavelength, about 1 cm. The peaks and valleys also remain at the same spanwise location.

As inclination was increased keeping q'' constant, it was found that spanwise variation arises earlier,

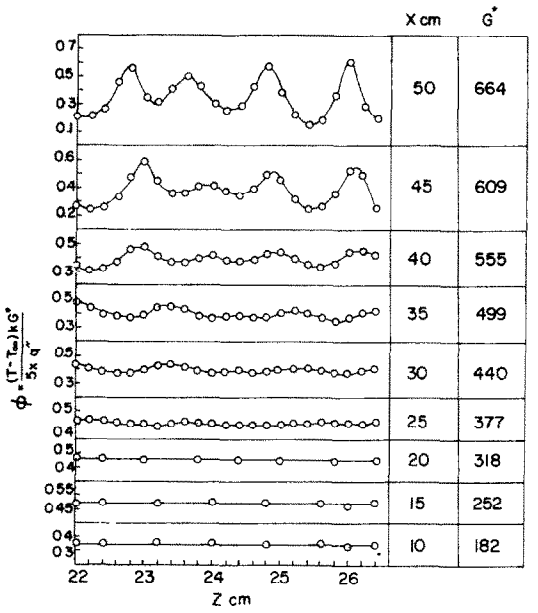

FIG. 2. Changing spanwise temperature distribution downstream at $y = 0.151$ cm, $q'' = 790$ W/m^2 and $\theta = 19°$.

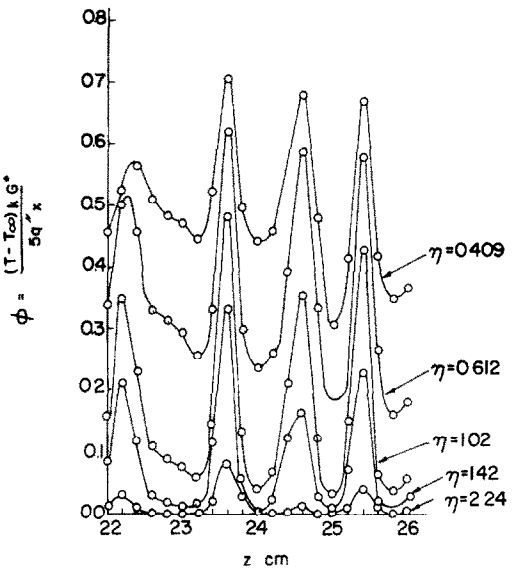

FIG. 3. Spanwise temperature variation across the boundary region at $x = 20$ cm for $q'' = 2294$ W/m^2, $G^* = 406$ and $\theta = 29°$.

and also remain almost spanwise-periodic with a constant wavelength. Further downstream the peaks and valleys shift in spanwise direction. During each measurement the thermocouple output at a given location was steady. Thus there were no periodic two-dimensional disturbances and the transverse pattern did not change with time. The same spanwise temperature variation is shown in Fig. 3 at various locations across the thermal region. The data were obtained at $x = 20$ cm, for $\theta = 29°$ and at higher flux. The variations are seen to extend to the outer edge of the thermal region, note the data at $\eta = 2.24$. The amplitude increases greatly as the surface is approached.

This time-independent pattern implies that stationary longitudinal vortices have been generated. They were first visualized by Sparrow and Husar [13]. The temperature peaks are positions between two adjacent vortices where the hot fluid is being expelled out from near the surface. The valleys lie at the intervening locations where the vortices are entraining cold ambient fluid. Thus, there is a pair of counter-rotating longitudinal vortices. Figure 2 implies a spatially stationary vortex pattern. However, at the larger angles they appeared to merge downstream.

Mean temperature distributions were determined across the thermal region at peak and valley. Data at three downstream locations are compared with the laminar solution in Fig. 4 for $\theta = 19°$. The agreement at $x = 20$ cm substantiates the practice of using only the parallel component of buoyancy force in the Grashof number. Further downstream the temperature profile changes. We note that at $x = 40$ cm the thermal region has become relatively thick at a peak and thin at a valley, consistent with the interactions with the ambient medium referred to above. These vortices are expected to also cause a local variation of surface temperature.

3.3. *Velocity measurements*

Typical measurements of the boundary region distribution of the streamwise velocity component, u, plotted as f', are shown in Fig. 5. The conditions are again those listed in Fig. 3. The spanwise variation is

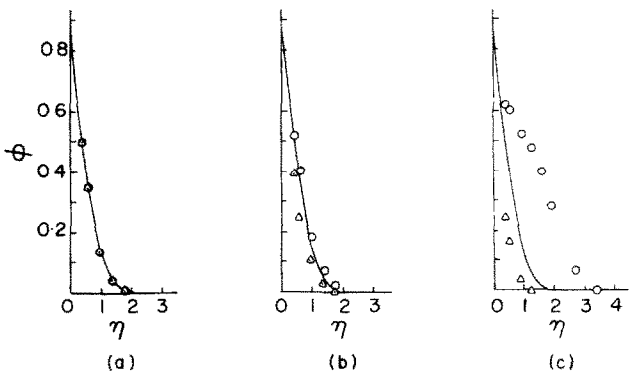

FIG. 4. Temperature distribution across the boundary layer at ⊙ peak, △ valley, $\theta = 19°$. (a) $x = 20$ cm and $G^* = 412$; (b) $x = 30$ cm and $G^* = 578$; (c) $x = 40$ cm and $G^* = 715$. Boundary-layer solution for vertical flow at $Pr = 6.0$.

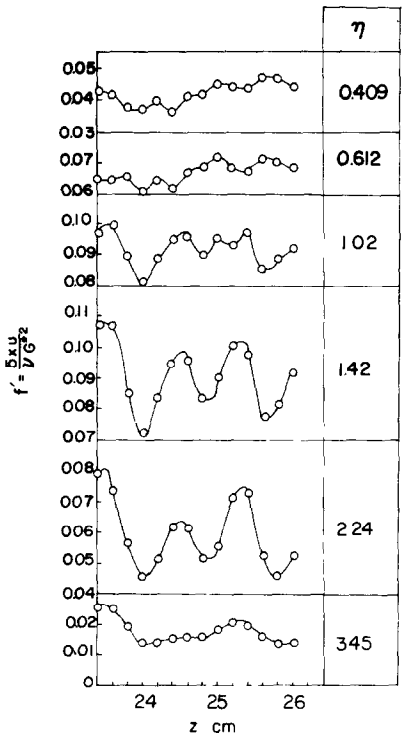

FIG. 5. Spanwise variation of the longitudinal velocity across the boundary layer. Conditions are the same as in Fig. 3.

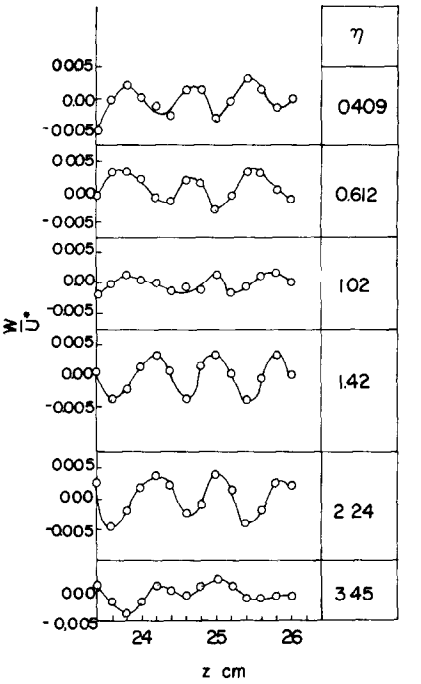

FIG. 7. Spanwise variation of the spanwise velocity across the boundary layer. Conditions are the same as in Fig. 3.

again periodic. It is in phase with the temperature variation, and is further consistent with the foregoing interpretation of vortex motion. The fluid moves outwards at peak and inwards at valleys.

The velocity profile across the boundary region, at a peak and valley are shown in Fig. 6 for the same conditions as in Fig. 4. At $x = 20$ cm the data are in good agreement with the laminar solution. Deviation arises further downstream. Again, there is the same thickening and thinning seen in Fig. 4. The profiles have shifted out and in at a peak and valley, respectively. This is again consistent with a vortex-ambient interaction.

Of greater interest is the distribution of the spanwise mean velocity component w. The distributions seen in Fig. 7 are also spanwise periodic. However, at about $\eta = 1$ there is a change in phase across the boundary region. This is seen very clearly in Fig. 8 where w is plotted across the boundary region at several spanwise locations. Each distribution is once positive and once negative across the flow layer. This is conclusive evidence of a single vigorous longitudinal vortex system in the boundary region.

Sparrow and Husar [13] had observed a single row of vortices over a uniform temperature inclined surface. Yet additional support for a single mechanism is the shifting of velocity profiles at a peak and valley, as noted in Fig. 6. However, the outer part of the mean velocity profiles does not show the steepening and flattening which is associated with a double row of vortices, see Audunson and Gebhart

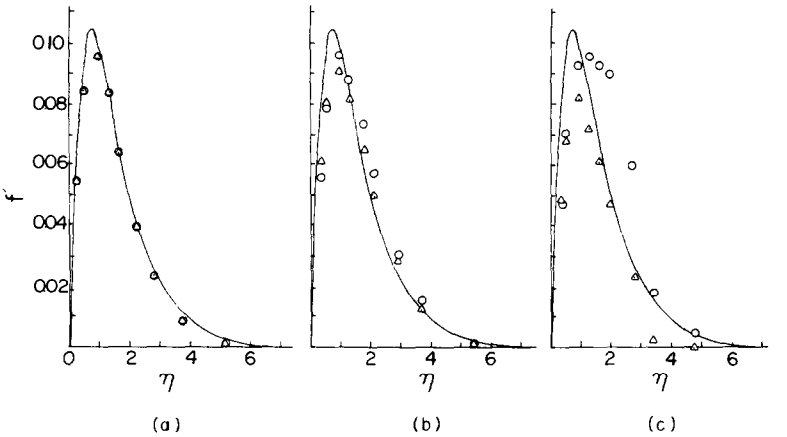

FIG. 6. Longitudinal velocity distribution across the boundary layer. Conditions are the same as in Fig. 4.

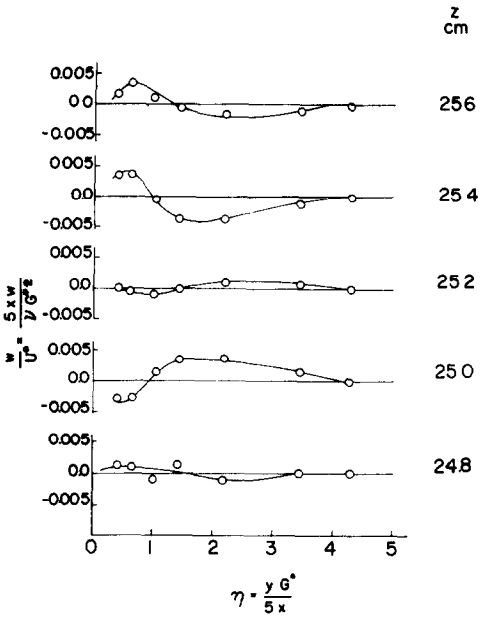

FIG. 8. Distribution of spanwise velocity across the boundary layer at different spanwise locations. Conditions are the same as in Fig. 3.

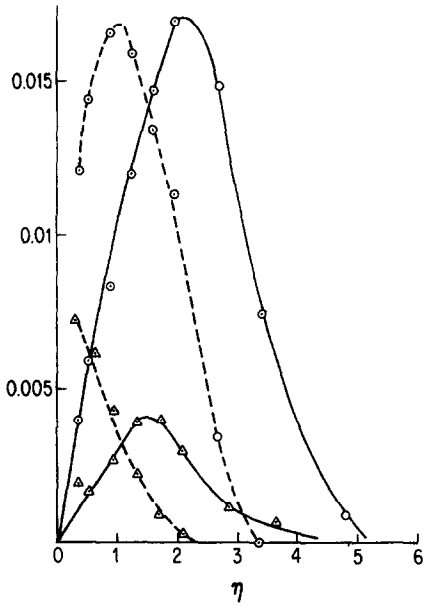

FIG. 9. Distribution of spanwise variations of temperature and velocity across the boundary region. $\theta = 19°$, △ $x = 30$ cm, $G^* = 578$, ⊙ $x = 40$ cm, $G^* = 715$. —— $\bar{f}_z'$, - - - $x\bar{\phi}_z'$

[24] and Jaluria and Gebhart [23]. The single system merely shifts the velocity profiles in and out from the surface.

3.4. *Distribution and growth of spanwise variations*

Typical root mean square values of spanwise variation of the temperature $\bar{\phi}_z'$ and longitudinal velocity $\bar{f}_z'$ are shown in Fig. 9 for two downstream locations in a given flow. The maximum temperature variation occurs near the surface and the peak moves out downstream. The disturbances also penetrate further out. Similar behavior is also observed for the spanwise variation of velocity.

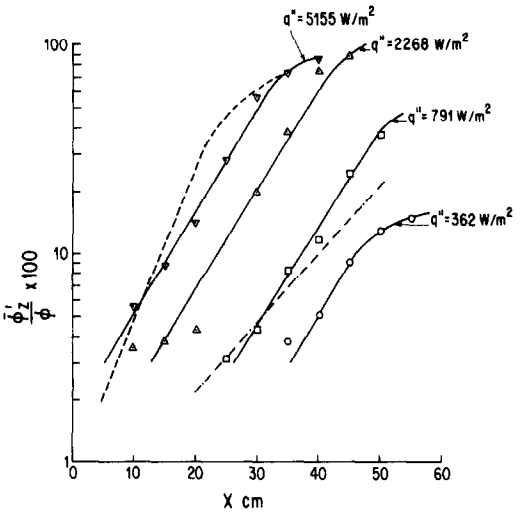

FIG. 10. Growth of spanwise temperature variation at $y = 0.151$ cm. - - - $\theta = 14°$, $q'' = 2250\,W/m^2$, —— $\theta = 19°$, – – – $\theta = 29°$, $q'' = 2303\,W/m^2$.

The downstream growth of spanwise temperature variation $\bar{\phi}_z'$ is shown as the solid curves in Fig. 10, for $\theta = 19°$ for four heat fluxes, at $y = 0.151$ cm. This is plotted as the ratio of RMS variation to the spanwise spatial average value $\bar{\phi}$. The initial growth rate is exponential and then tapers off downstream. Similar trends and growth were found for velocity. In Fig. 10 we also show the growth rates at approximately the same flux for different inclinations. The growth rate is seen to increase with inclination.

3.5. *Vortex wave length*

The experiments of Sparrow and Husar [13] indicate that the longitudinal vortex wavelength in flow over an isothermal surface is independent of the angle of inclination, but depends on the difference between the surface and ambient temperature. Lloyd [15] found this dependence to be of the form

$$\lambda \propto (T_0 - T_\infty)^{-0.19}.$$

With a uniform flux this temperature difference is not constant along the surface, but increases as $T_0 - T_\infty \propto x^{0.2}$ in laminar flow. For our uniform flux surface we also found that wavelength was independent of inclination. However, it depends on heat flux as $\lambda = 1.27 q''^{-0.12}$ with a root mean square deviation of 3% in the range $362 \leqslant q'' \leqslant 7094\,W/m^2$. The wavelength of the vortices also does not change downstream. Recall Fig. 2.

Our measured wavelengths are tabulated in Table 1 and also plotted as points in Fig. 11 on the stability plane of Haaland and Sparrow [18], calculated for an isothermal surface and $Pr = 6.7$. A similar plant for uniform flux boundary condition is not yet available. For flow generated by a vertical surface, subjected to two-dimensional disturbances, Knowles [31] has shown that the neutral stability curve for an isothermal condition is contained within

Table 1. Experimental values of beginning of spanwise variation and vortex wave length

θ	x cm	q'' W/m^2	λ cm	Pr	G^*
14°	42.0	797	0.55	6.2	592
14°	31.0	2250	0.50	6.1	581
14°	18.0	5127	0.48	5.4	473
14°	13.0	7094	0.44	5.1	403
19°	40.5	362	0.70	6.3	483
19°	31.0	791	0.56	6.4	452
19°	17.2	2268	0.53	6.0	364
19°	9.8	5147	0.48	5.7	282
29°	22.8	363	0.63	6.7	288
29°	17 3	790	0.57	6.4	281
29°	9.4	2303	0.53	6.1	220

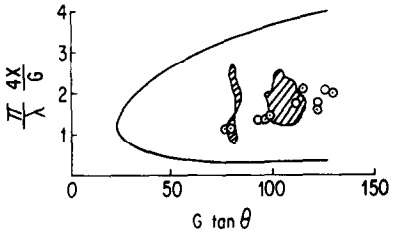

FIG. 11. Neutral stability diagram from Haaland and Sparrow [18]. ⊙ Present data. Shaded areas are the data of Lloyd [15].

that for uniform flux. Perhaps this also results for an inclined surface. The stability plane in Fig. 11 is plotted in terms of $4\pi x/\lambda G$ vs $G\tan\theta$ where $G = 2(2)^{1/2}[g\beta(T_0 - T_\infty)x^3/\nu^2]^{0.25}$. We convert our values of G^* to G using relation $G^* = 1.28G$ given in Knowles [31] and Jaluria and Gebhart [26]. Our data points are in the unstable region, and in close agreement with the collection of the data of Lloyd [15]. Note that Haaland and Sparrow have used the wavelength of spanwise disturbance variation in their analysis. This is twice of vortex wavelength.

3.6. *Beginning of transition*

Many earlier investigators [2, 4–6, 8, 12] have attempted to locate the point where the laminar flow ends. Each of these authors have given a location of the point where laminar flow ends, according to their criterion, in terms of Rayleigh number. Lloyd and Sparrow [14] have compared these values from all the studies previous to theirs. Such data was found to be scattered about a decade on either side of theirs, except for that of Tritton [32], which was four decades lower. We note that Tritton's experimental configuration was more like a channel. Subsequent investigators have compared their data with that of Lloyd and Sparrow [14] and found it to be within the scatter of most data.

The criterion of Jaluria and Gebhart [26] may be expressed as

$$E = G^*\left(\frac{\nu^2}{gx^3}\right)^{2/15}.$$

The value of E from their experiments on a uniform-flux vertical surface was found to be 13.6 and 15.2 for the beginning of velocity and thermal transition, respectively. Transition data from other studies were within an E range from 12.6 to 24.0. These data are for gases and liquids, over a range of Prandtl number from 0.7 to 11.85, for both isothermal and uniform flux surface conditions.

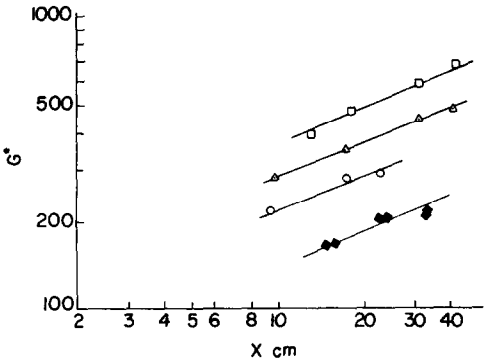

FIG. 12. Beginning of spanwise variation for angles ⊙ 29°, △ 19°, ⊡ 14°. Also shown are results of Hassan and Mohamed [4] at 60°, ◆.

In this study we specify that transition has begun locally downstream, when the root mean square value of spanwise temperature variation becomes 5% of the mean value. The values of x where picked from plots such as Fig. 10 and are plotted in terms of G^* vs x in Fig. 12. Data are shown for $\theta = 14$, 19 and 29°. The lines match very well the trends of the data. The resulting average values of E was correlated by $E = 88\theta^{-0.65}$, where θ is in degrees and in the range $9° \leqslant \theta \leqslant 30°$.

During these experiments it was possible to locate the conditions wherein time-periodic disturbances arose. They were determined as the point where peak to peak value of these disturbances becomes 5% of the average value. These were correlated in the form $E = 21\ (1 - \theta/120)$ where θ is again in degrees from vertical. The data and these two correlations suggest, for inclinations greater than about 11°, that spanwise variations occur first and then are followed downstream by time-periodic disturbances. The difference between these two locations, in terms of E, decreases with angle. At around 10° the two levels occur simultaneously. For isothermal surface, Lloyd and Sparrow [14] found that the two coexist between 15 and 17°.

Most of earlier data for transition in inclined flows is reported in terms of Rayleigh numbers. Seldom is enough information provided to calculate E factor, for comparison with our results. The exceptions are the data of Vliet [3] and Hassan and Mohamed [4]. The latter data is for an isothermal surface in air and detailed data is given for inclinations to 60° from vertical. Their data for transition, according to their criterion, are also shown in Fig. 12. Grashof numbers were calculated and converted to G^* by using the relationships given in Knowles [31] as $G^* = 1.12G$ for air. The resulting average E is 15 and the trend is similar to present data.

The transition data of Vliet [3] at inclinations of 5, 15, 30, 45 and 60° were also plotted as in Fig. 12.

However, a similar regular ordering did not arise. There was large scatter and no definite trend of G^* variation with x was found. This may be explained as follows. We have shown that the presence of vortices on an inclined surface causes a substantial spanwise variation of temperature in the flow. This results in a spanwise variation of surface temperature, for a uniform flux surface. The surface temperature at a peak will be higher than at a valley. Vliet [3] measured the surface temperature along the physical centerline of the surface, independent of the pattern of the flow. If vortex entrainment of cold fluid happens to occur there, then the surface temperature will be lower than average. Thus, a single local measurement cannot give a reliable indication of transition. Hassan and Mohamed's data, on the other hand, was averaged over the span of the surface.

3.7. *Disturbance frequency*

Experiments and analysis have shown that a vertical natural convection boundary-layer flow filters disturbances for essentially a single, or characteristic, frequency downstream, see Gebhart and Mahajan [33]. Data from the present experiment, with the surface vertical, was shown by these authors to be within $\pm 8\%$ of predicted values. We also have frequency data for time periodic disturbances which appeared in our inclined flows. The frequencies, locations and conditions are collected in Table 2.

Table 2. Experimental values of beginning of time-periodic disturbances and characteristic frequency B^*

θ	x cm	q″ W/m²	f Hz	Pr	G^*	B^*
14°	40.0	2250	0.36	6.0	715	0.74
14°	25.0	5127	0.55	5.4	620	0.70
14°	20.0	7094	0.67	5.0	575	0.69
19°	35.0	2269	0.43	6.0	664	0.63
19°	25.0	5147	0.60	5.5	606	0.74
29°	25.0	2303	0.33	6.2	477	0.73

The resulting values of B^* are remarkably close to the values of $B^* = 0.675$ for vertical flow and $Pr = 6.7$ given in Gebhart and Mahajan [33].

3.8. *Some additional general observations.*

For a vertical surface, the entrainment velocity v_∞ is near horizontal. Taking typical values of $G^* = 800$ and $x = 30$ cm, we calculate from laminar theory that v_∞ is of the order of 0.05 cm/s in water. Calibrations of a hot-film at low velocities when the flow direction is near horizontal have shown that there is a lower limit of velocity below which a single heated sensor may not be used. See Shaukatullah [28]. In addition the direction of flow must in general be known for flow at other angles, because of the mixed convection effect. The lower limit for near horizontal flow for the film probes used in this study, was found to be 0.22 cm/s. Thus, our velocity measurements at the edge of the boundary layer are not expected to be very reliable. In fact we found that as the probe approaches the edge of the boundary layer the output of the anemometer becomes less than with zero velocity. This effect of flow direction is explained in [28].

The size of the vortices found in this study were of the order of 0.5 cm. The two hot films spanned almost this distance. Since the vortices were stationary and the flow was steady upstream, it was possible to account for spatial separation by correctly located traverses in the spanwise direction. However, such a probe configuration cannot be used to measure fluctuating components of velocity in vortices of this size. The measurement must approach instantaneous values at the same location. This is not even approximately achieved by our configuration.

4. CONCLUSIONS

Our detailed temperature and velocity measurements have indicated conclusively that a single mean flow longitudinal vortex system arises. It substantially modifies the distributions of temperature and velocity. The spanwise variation is almost periodic upstream. Its consequence is a spanwise variation in surface temperature. For angles greater than 11° the spanwise variation occurs first downstream, followed yet further downstream by appreciable two dimensional periodic disturbances. At about 10° inclination both disturbance forms appear at about the same location downstream. For angles less than 9° the spanwise variation does not become appreciable.

For our uniform flux surface the wavelength of the spanwise variations is independent of angle but depends on the heat flux level. Although there has been no stability analysis for a uniform-flux surface condition, our results are qualitatively in agreement with the analysis for an isothermal surface condition. Initially the amplitude growth rate of these variations is found to be exponential. An analogous phenomenon, known as Gortler–Taylor vortices, occurs in forced flow on a concave wall. There it is found that the vortex wavelength is nearly independent of free stream velocity and depends on the radius of curvature. See Tani [34].

The location of the beginning of both spanwise and two-dimensional disturbances was found to depend on x in addition of G^*. This interdependence was correlated by the E factor of Jaluria and Gebhart [26], which arise for vertical flows. The data of Hassan and Mohamed [4] on inclined surface also showed similar trends.

Acknowledgements—The experimental work reported here was done at Cornell University. It is a pleasure to acknowledge the assistance of the Technical Services Facility in Upson Hall and Mr. J. Farrara of Dodge Industries, Hoosick Falls, New York in building the apparatus. Mrs. Bonnie Boskat of SUNYAB typed the manuscript. Financial support was under NSF grants GK-18529, ENG-75 05466 and ENG-75 22623.

REFERENCES

1. E. Schmidt, Schlierenaufnahmen des Temperaturfeldes in der Nahe warmeabgebender Korper, *Forsch. Geb. Ingwes.* **3**, 1818–1819, (1932).
2. B. R. Rich, An investigation of heat transfer from an inclined flat plate in free convection, *Trans. Am. Soc. Mech. Engrs* **75**, 489–499 (1953).
3. G. C. Vliet, Natural convection local heat transfer on constant-heat-flux inclined surface, *J. Heat Transfer* **91C**, 511–516, (1969).
4. K. -E. Hassan and S. A. Mohamed, Natural convection from isothermal flat surfaces, *Int. J. Heat Mass Transfer* **13**, 1873–1886 (1970).
5. J. R. Lloyd, E. N. Sparrow and E. R. G. Eckert, Laminar, transition and turbulent natural convection adjacent to inclined and vertical surfaces, *Int. J. Heat Mass Transfer* **15**, 457–473 (1972).
6. T. Fujii and H. Imura, Natural-convection heat transfer from a plate with arbitrary inclination, *Int. J. Heat Mass Transfer* **15**, 755–767 (1972).
7. G. C. Vliet and D. C. Ross, Turbulent natural convection on upward and downward facing inclined constant heat flux surfaces, *J. Heat Transfer* **97C**, 549–555 (1975).
8. W. Z. Black and J. K. Norris, The thermal structure of free convection turbulence from inclined isothermal surfaces and its influence on heat transfer, *Int. J. Heat Mass Transfer* **18**, 43–50 (1975).
9. W. T. Kierkus, An analysis of laminar free convection flow and heat transfer about an inclined isothermal plate, *Int. J. Heat Mass Transfer* **11**, 241–253 (1968).
10. N. Riley, Note on a paper by Kierkus, *Int. J. Heat Mass Transfer* **18**, 991–993 (1976).
11. J. B. Lee and G. S. H. Lock, Laminar boundary layer free convection along an inclined isothermal surface, *Trans. Can. Soc. Mech. Engrs* **1**, 189–196 (1972).
12. G. S. H. Lock, C. Gort and G. R. Pond, A study of instability in free convection from an inclined plate, *Appl. Scient. Res.* **18**, 171–182 (1967).
13. E. M. Sparrow and R. B. Husar, Longitudinal vortices in natural convection flow on inclined plates, *J. Fluid Mech.* **37**, 251–255 (1969).
14. J. R. Lloyd and E. M. Sparrow, On the instability of natural convection flow on inclined plates, *J. Fluid Mech.* **42**, 465–470 (1970).
15. J. R. Lloyd, Vortex wavelength in the transition flow adjacent to upward facing inclined isothermal surfaces, in *Heat Transfer* 1974, Vol. 3, Paper No. NCl.8, 34–37, Proceedings of the Fifth International Heat Transfer Conference, Tokyo (1974).
16. J. B. Lee and G. S. H. Lock, Instability in boundary-layer free convection along an inclined plate, *Trans. Can. Soc. Mech. Engrs* **1**, 197–203 (1972).
17. S. E. Haaland and E. M. Sparrow, Wave instability of natural convection on inclined surfaces for nonparallelism of the basic flow, *J. Heat Transfer* **95C**, 405–407 (1973).
18. S. E. Haaland and E. M. Sparrow, Vortex instability of natural convection flow on inclined surfaces, *Int. J. Heat Mass Transfer* **16**, 2355–2367 (1973).
19. G. J. Hwang and K. C. Cheng, Thermal instability of laminar natural convection flow on inclined isothermal plates, *Can. J. Chem. Engng*, **51**, 659–666 (1973).
20. P. A. Iyer and R. E. Kelly, The stability of the laminar free convection flow induced by a heated inclined plate, *Int. J. Heat Mass Transfer* **17**, 517–525 (1974).
21. R. A. Kahawita and R. N. Meroney, The vortex mode of instability in natural convection flow along inclined plates, *Int. J. Heat Mass Transfer* **17**, 541–548 (1974).
22. B. Gebhart, Natural convection flows and stability, in *Advances in Heat Transfer*, edited by T. F. Irvine and J. P. Hartnett, Vol. 9, pp. 273–348. Academic Press, New York (1973).
23. Y. Jaluria and B. Gebhart, An experimental study of nonlinear disturbance behaviour in natural convection, *J. Fluid Mech.* **61**, pp. 337–365 (1973).
24. T. Audunson and Gebhart, Secondary mean motions arising in a buoyancy induced flow, *Int. J. Heat Mass Transfer* **19**, 737–750 (1976).
25. F. Godaux and B. Gebhart, An experimental study of natural convection flow adjacent to a vertical surface, *Int. J. Heat Mass Transfer* **17**, 93–107 (1974).
26. Y. Jaluria and B. Gebhart, On transition mechanism in vertical natural convection flow, *J. Fluid Mech.* **66**, 309–337 (1974).
27. G. C. Vliet and C. K. Liu, An experimental study of turbulent natural convection boundary layers, *J. Heat Transfer* **91C**, 517–531 (1969).
28. H. Shaukatullah, An experimental investigation of the natural convection boundary layer over a uniform flux inclined surface, Ph.D. Dissertation, Cornell University, Ithaca, New York (1977).
29. G. S. Kell, Thermodynamic and transport properties of fluid water, in *Water—A Comprehensive Treatise*, edited by F. Franks. Plenum Press, New York (1972).
30. C. A. Meyers, R. B. McKlintock, G. J. Silvestri and R. C. Spencer, *Steam Tables*, 2nd Edn. ASME, New York (1968).
31. C. P. Knowles, A theoretical and experimental study of the stability of the laminar natural convection boundary layer over a vertical uniform flux plate, Ph.D. Dissertation, Cornell University, Ithaca, New York (1967).
32. D. J. Tritton, Transition to turbulence in free convection boundary layers on an inclined heated plate, *J. Fluid Mech.* **16**, 417–435 (1963).
33. B. Gebhart and R. Mahajan, Characteristic disturbance frequency in vertical natural convection flow, *Int. J. Heat Mass Transfer* **18**, 1143–1148 (1975).
34. I. Tani, Production of longitudinal vortices in the boundary layer along a concave wall, *J. Geophys. Res.* **68**, 3075–3080 (1962).

ETUDE EXPERIMENTALE DE LA CONVECTION NATURELLE SUR UNE SURFACE INCLINEE

Résumé—Un thermocouple et deux sondes anémométriques à fil chaud en forme de V renversé sont utilisés pour explorer l'écoulement sur une surface inclinée dissipant un flux thermique uniforme. On mesure la température et les composantes longitudinale et transversale de vitesse. Il se forme un système de tourbillons longitudinaux. Cela occasionne une variation latérale des champs de température et de vitesse, et donc du transfert thermique. La variation latérale de l'écoulement moyen, ou du système de tourbillons, apparait pour des angles supérieurs à 11°. Des mesures locales permettent des comparaisons détaillées avec les mécanismes bien établis de perturbation dans les écoulements verticaux. On trouve encore le filtrage en fréquence de perturbations périodiques. Le début de la transition est postulé en termes d'amplitude de perturbation. La localisation est trouvée dépendre de la distance du bord d'attaque, en plus du nombre de Grashof, de la même façon que dans les écoulements verticaux.

EINE EXPERIMENTELLE UNTERSUCHUNG DER STRÖMUNG BEI FREIER KONVEKTION AN EINER GENEIGTEN OBERFLÄCHE

Zusammenfassung—Ein Thermoelement und zwei Hitzdrahtanemometersonden in Form eines "umgekehrten V" wurden benutzt, um die Strömung im Grenzschichtbereich zu untersuchen, die sich über einer geneigten Oberfläche bei gleichförmiger Wärmestromdichte ausbildet. Temperatur, Längs- und Querkomponmenten der Geschwindigkeit wurden gemessen. Ein einzelnes Wirbelsystem entsteht in Längsrichtung. Es verursacht eine abschnittsweise Variation des Temperatur- und Geschwindigkeitsfeldes wodurch sich eine abschnittsweise Variation der Wärmeübertragung ergibt. Die abschnittsweise Variation der mittleren Strömung oder des Wirbelsystems entsteht zuerst stromabwärts bei Winkeln größer als 11 Grad. Unsere örtlichen Messungen erlauben einen detaillierten Vergleich mit wohlbekannten Störungsmechanismen bei vertikalen Strömungen. Die Frequenzfilterung von periodischen Störungen wurde wieder beobachtet. Der Beginn des Übergangs wird als von der Größe der Störung abhängig vorausgesetzt. Es wird gefunden, daß der Umschlagpunkt, ähnlich wie bei vertikalen Strömungen, außer von der Grashof–Zahl auch vom Abstand von der Anströmkante abhängt.

ЭКСПЕРИМЕНТАЛЬНОЕ ИССЛЕДОВАНИЕ СВОБОДНОКОНВЕКТИВНОГО ТЕЧЕНИЯ НА НАКЛОННОЙ ПОВЕРХНОСТИ

Аннотация — Для исследования течения в пограничном слое на наклонной равномерно нагреваемой поверхности использовались термопара и два пленочных термоанемометра в виде перевернутой буквы V. Измерялись температура, а также продольная и поперечная компоненты скорости. В эксперименте наблюдалось образование единичной системы продольных вихрей, которая вызывала изменение полей температуры и скорости по ширине потока, что в свою очередь приводило к изменению теплоотдачи по поверхности. Система вихрей возникала вначале в нижней части пластины, когда угол её наклона превышал 11°. Локальные измерения позволили провести детальное сопоставление с хорошо разработанными механизмами возникновения возмущений при обтекании вертикальных поверхностей. Подтверждена частотная фильтрация периодических возмущений. Обнаружено, что начало переходного режима связано с величиной возмущений. Как и при обтекании вертикально расположенных поверхностей место возникновения перехода зависит от числа Грасгофа и расстояния от передней кромки.